HHS Public Access

Author manuscript

Mucosal Immunol. Author manuscript; available in PMC 2016 May 18.

Published in final edited form as:

Mucosal Immunol. 2016 January ; 9(1): 38–55. doi:10.1038/mi.2015.34.

Macrophages are critical to the maintenance of IL-13-dependent lung inflammation and fibrosis

Lee A. Borthwick[1,2,*], **Luke Barron**[2,*], **Kevin M. Hart**[2], **Kevin M. Vannella**[2], **Robert W. Thompson**[2], **Sandra Oland**[2], **Allen Cheever**[2], **Joshua Sciurba**[2], **Thirumalai R. Ramalingam**[2], **Andrew J. Fisher**[1,3], and **Thomas A. Wynn**[2,#]

[1]Tissue Fibrosis and Repair Group, Institute of Cellular Medicine, Medical School, Newcastle University, Newcastle Upon Tyne, NE2 4HH, UK

[2]Immunopathogenesis Section, Laboratory of Parasitic Diseases, National Institute of Allergy and Infectious Diseases, National Institutes of Health, Bethesda, MD, USA

[3]Institute of Transplantation, Freeman Hospital, High Heaton, Newcastle Upon Tyne, NE7 7DN, UK

Abstract

The roles of macrophages in type 2-driven inflammation and fibrosis remain unclear. Here, using CD11b-Diphtheria Toxin Receptor (DTR) transgenic mice and three models of IL-13-dependent inflammation, fibrosis, and immunity, we show that $CD11b^+$ $F4/80^+$ Ly6C+ macrophages are required for the maintenance of type-2 immunity within affected tissues but not secondary lymphoid organs. Direct depletion of macrophages during the maintenance or resolution phases of secondary *S. mansoni* egg-induced granuloma formation caused a profound decrease in inflammation, fibrosis, and type-2 gene expression. Additional studies with CD11c-DTR and CD11b/CD11c-DTR double transgenic mice suggested that macrophages but not dendritic cells were critical. Mechanistically, macrophage depletion impaired effector $CD4^+$ Th2 cell homing and activation within the inflamed lung. Depletion of $CD11b^+$ $F4/80^+$ $Ly6C^+$ macrophages similarly reduced house dust mite-induced allergic lung inflammation and suppressed IL-13-dependent immunity to the nematode parasite *Nippostrongylus brasiliensis*. Consequently, therapeutic strategies targeting macrophages offer a novel approach to ameliorate established type-2 inflammatory diseases.

Introduction

Type 2 cytokine responses are important drivers of tissue remodelling and fibrosis in many diseases, including asthma, ulcerative colitis and chronic helminth infections[1–3]. In all these diseases, the affected organs accumulate a heterogeneous population of macrophages

[#]Corresponding Author: Dr Thomas A Wynn, Laboratory of Parasitic Diseases, National Institute of Allergy and Infectious Diseases, National Institutes of Health, Bethesda, MD, Tel. - 301-496-4758, Fax. - 301-480-5025, ; Email: twynn@niaid.nih.gov

[*]These authors contributed equally to this work

The authors declare no conflicts of interest.

derived from recruited monocytes and activated tissue residents whose phenotype shifts as the inflammatory response progresses. Many recent studies have cumulated in two key conclusions: that the origins and homeostatic signals for resident tissue macrophages and monocyte-derived macrophages differ fundamentally, and that monocytes are capable of developing multiple distinct phenotypes and functions when entering tissues[4–9]. Macrophage depletion studies have identified no defects in systemic initiation of type 2 cytokine responses during helminth infection[10–12]. However, their overall role in maintaining or resolving established IL-13-driven inflammation and fibrosis has not been examined.

To dissect the role of macrophages in type 2 immunity in the lung, we examined three models of Th2-associated disease and, rather than targeting a single signalling pathway or putative effector gene, we transiently depleted macrophages using CD11b-Diphtheria Toxin Receptor (CD11b-DTR) transgenic mice treated with diphtheria toxin (DTX)[13,14]. This well-established model offers the advantage of selectively depleting monocytes, monocyte descendants, and most tissue macrophages independently of their phagocytic activity and without impacting CD11b+ eosinophils, neutrophils, or other innate populations[10,13–18]. Our primary model was intravenous challenge of antigen-primed mice with *Schistosoma mansoni* eggs, creating eosinophil-rich fibrotic granulomas in the lung which progress through characteristic stages. We also employed acute house dust mite (HDM)-induced allergic airway inflammation and infection with *Nippostrongylus brasiliensis*, a hookworm parasite that migrates destructively through the lung and resides in the small intestine before being expelled by IL-13-dependent mechanisms.

Unexpectedly, the combined data from all three models revealed a striking decrease in type 2-dependent inflammation and fibrosis in the lung, without impaired IL-13 responses in draining lymph nodes, regardless of when macrophages were depleted. In contrast to previous studies based on chemical or surgical injury suggesting macrophages switch from pro- to anti-fibrotic roles between the initiation and resolution phases of liver fibrosis [13,15,19], we show that macrophages exhibit pro-fibrotic activity at all stages of the IL-13-driven inflammatory response in the lung. Mechanistically, we found that macrophages play a critical role in recruiting and activating effector $CD4^+$ Th2 cells in the affected tissues which likely explains why depleting macrophages rapidly decreases IL-13-dependent lung fibrosis. An important implication of our findings is that IL-13-driven tissue inflammation and fibrosis can resolve rapidly if macrophages are rendered incapable of recruiting T cells and actively maintaining tissue-localized immune responses. Therefore, therapeutic strategies that deactivate macrophages or reverse their accumulation in inflamed tissues could emerge as viable targets to ameliorate progressive IL-13-driven fibrosis and other diseases associated with persistent overproduction of type 2 cytokines.

Results

Macrophages are critical to maintain IL-13-dependent lung inflammation and fibrosis

When injected intravenously, *S. mansoni* eggs lodge in lung capillaries and induce a vigorous eosinophil-rich granulomatous type 2 immune response, which leads to the activation of collagen-producing myofibroblasts, deposition of excess extracellular matrix,

and IL-13-dependent fibrosis[20,21]. We examined whether the induction, maintenance or resolution of secondary granulomatous inflammation and pulmonary fibrosis induced by *S. mansoni* depends on macrophages.

We first confirmed peritoneal and lung macrophages from CD11b-DTR mice were sensitive to DTX-induced death *in vitro* and *in vivo* within 18 hours (Fig. 1, S1). To determine which inflammatory cell types were directly targeted by DTX, we treated egg primed and challenged CD11b-DTR mice with a single dose of DTX on day 3 post-challenge and ~18 hours later analyzed lung leukocyte populations. A single dose of toxin depleted ~50% of CD11b+ F4/80+ macrophages (Fig. 1a–b). By contrast, the number of total lung leukocytes, eosinophils, neutrophils, or T cells did not immediately decrease. Macrophages outnumbered dendritic cells (DCs) by ~20-fold, and neither CD11b+ nor CD11b− DCs (as defined by CD11c+ MHCII+ F4/80− gates) were directly reduced by DTX treatment. Such incomplete but preferential depletion of macrophages, without a direct net loss of all types of CD11b+ inflammatory leukocytes, is a useful feature of the CD11b-DTR mice and our results match those described in a variety of models[10,13–18].

The immune response to *S. mansoni* eggs generates granulomas in stages[21]. Innate immunity initiates granuloma formation, then between days 4 and 7 adaptive immunity amplifies the response and granulomas reach their peak size and develop a fibrotic perimeter, predominantly driven by IL-13 from Th2 cells. Inflammation is resolving by day 14. We designed experiments to deplete macrophages during the initiation, peak, and resolution stages of a secondary type-2 inflammatory response (Fig. 2a). In these studies, depleting macrophages after challenging either naïve (primary) or egg-sensitized (secondary) mice with live *S. mansoni* eggs reduced granuloma volume on both day 4 and 7 (Fig. 2b–d, Fig. S2). Surprisingly, although macrophages are necessary for the resolution of sterile inflammation and fibrosis[13,19], depletion after the peak of the response dramatically reduced fully established granulomatous inflammation by day 14.

Indeed, the granulomas measured on day 14 in DTX treated mice were even smaller than those measured on day 4 when secondary granulomas were first forming. Total lung collagen content did not change during the first 4 days after *S. mansoni* egg challenge in antigen-primed mice but increased by ~50% on day 7 and nearly ~100% by day 14 (Fig. 2e). Depletion of macrophages significantly inhibited the increase in lung collagen on day 7 and 14 as determined by both hydroxyproline content (Fig. 2e) and picrosirius red staining (Fig. 2f). These results demonstrate that during a secondary granulomatous response, macrophages are critically required at all time points to maintain type 2 cytokine driven inflammation and fibrosis within the lung.

Type 2 immunity in the granulomatous lung is dependent on macrophages

IL-12, IFN-γ, iNOS, and IL-10 have each been shown to negatively regulate *S. mansoni* egg-induced type 2 pathology[20,22,23]. Therefore, we examined whether the decreases in inflammation and fibrosis observed in the DTX-treated animals were a result of changes in type 1 or regulatory gene expression. Little to no change in *Il12b* or *Ifng* expression was observed and *Il10* was similarly increased in both treatment groups (Fig. 3a). In addition, although *Nos2* exhibited anti-fibrotic activity in a related model[23], we observed decreased

Nos2 expression on days 7 and 14 following DTX treatment (Fig. 3a) likely because macrophages are major producers of inducible nitric oxide. Therefore, counter-regulation of Th2 cytokine responses by these negative regulators could not explain why depleting macrophages reduced inflammatory pathology.

T cell-derived IL-4 and IL-13 are the critical cytokines regulating granuloma development, while IL-13 functions as they key mediator of fibrosis [24–26]. Therefore, we also examined whether the type 2 immune response in the lung was altered following depletion. In agreement with the marked reductions in granuloma size and fibrosis, we found that expression of type 2 cytokines (*Il13, Il5*) and several type 2 inducible genes (*Retnla*, *Chi3l3*, *Arg1*, *IL13ra2*) were decreased at all time points (Fig. 3b). In contrast, *Arg2* expression, which is not regulated by the type 2 immune response, was unaffected. Interestingly, depletion only slightly altered expression of *Il13ra1*in the lungs, whereas expression of the IL-4/IL-13-inducible IL-13 decoy receptor (*Il13ra2*) was blunted substantially, further supporting a marked reduction in type 2 immunity against *S. mansoni* eggs (Fig. 3b). Moreover, depletion caused similar changes to the pattern of gene expression in the lungs of mice challenged with eggs without priming (Fig. S3).

Depletion of macrophages in the granulomatous lung indirectly reduces inflammation

The pattern of Th2-induced gene expression in the lungs reaches a maximum between days 4 and 7, as granuloma formation peaks. DTX treatment notably impaired this second step of T cell-driven amplification (Fig. 3b). Therefore, we next treated egg sensitized and challenged mice with DTX on days 3, 4, and 5 post-challenge and analyzed changes in lung inflammation on day 7. Between days 4 and 7 the direct depletion of macrophages indirectly and cumulatively reduced the number of lung leukocytes in general, including eosinophils, T cells, and both CD11b+ and CD11b− DCs, but with the exception of neutrophils (Fig. 4a). This overall reduction in inflammation was accompanied by a dramatic change in the phenotype of the remaining lung macrophages (Fig. 4b–c). In control mice the fraction of Ly6C+ macrophages, likely recently recruited monocytes, diminished between days 4 and 7 whereas expression of CD64, CD11c, and MHCII, and the total number of macrophages, were maintained. In DTX-treated mice, the remaining population of CD11b+ F4/80+ macrophages expressed high levels of Ly6C and CD64 but little CD11c or MHCII, suggesting new monocytes quantitatively but not qualitatively replenished depleted lung macrophages within 2 days. Together these data (Fig. 1, Fig. 4) show that DTX caused direct but incomplete depletion of CD11b+ F4/80+ macrophages in the lung without reducing other leukocyte populations. Yet, even partial macrophage depletion was sufficient to indirectly and cumulatively reduce overall lung inflammation within 3 days corresponding with the substantial loss of CD11c− and MHCII-expressing F4/80+ cells and, within 2 days of the final DTX treatment, their replacement by cells resembling conventional monocytes.

Reduced local but not systemic CD4$^+$ Th2 cell responses underlie decreased lung inflammation and fibrosis

Since IL-13 and IL-5 were reduced in whole lung tissue (Fig. 3b), we next examined helper T cell activation, differentiation, and homing. Importantly, DTX treatment did not reduce the percentage (Fig. 5a), number (not shown), or magnitude of expression (Fig. S4) of IL-13 and

IL-4 by $CD4^+$ T cells in the lung-draining mediastinal lymph nodes at any time point. Instead, we found small but highly consistent decreases in the percentages and greater reduction in the numbers of IL-13 and IL-4 producing $CD4^+$ T cells in the lung, and diminished cytokine production on a per-cell basis (Fig. 5b–d). In contrast, IFN-γ was unchanged in either the lung or mediastinal lymph nodes, while IL-17A increased in the lymph nodes but decreased in the lung (Fig. 5, Fig. S4). Experiments with unprimed mice yielded similar results (Fig. S5, not shown). Together, these results imply that macrophage depletion does not interfere with T cell priming in lymph nodes, but once the type 2 response is established macrophages play a critical role in recruiting, reactivating, and/or retaining the effector Th2 cell response in the lung.

Targeted depletion of DCs after antigen priming and egg challenge does not reduce type 2-dependent granulomas and fibrosis in the lung

The successful generation of cytokine-producing CD4 T cells in lymph nodes suggested that sufficient antigen presentation still occurred outside the lungs in DTX-treated CD11b-DTR mice (Fig. 5a, Fig. S4, Fig. S5), and the numbers of CD11b+ DCs in the lung did not immediately change when half the macrophages were depleted (Fig. 1b). Nonetheless, it is both plausible and of obvious importance that CD11b+ DCs might also be partially susceptible to depletion in our experiments, and the cumulative effects of DTX treatment include a delayed drop in the number of DCs present in lung and draining lymph node (Fig. 4, Fig. S6.). Therefore, we compared our findings to the effect of targeting DCs for depletion using the CD11c-DTR system. Unlike CD11b-DTR mice, CD11c-DTR mice die 2–3 days after DTX injection due to toxic neurological effects on transgene-expressing non-hematopoietic cells[27]. In order to study fibrosis, we generated bone marrow chimeras in which wild-type recipient mice received wild-type control, CD11b-DTR, CD11c-DTR, or CD11b/c-DTR double-transgenic donor bone marrow. Egg-sensitized chimeric mice were challenged IV with live *S. mansoni* eggs and then treated with DTX on days 3, 4, and 5 to deplete different leukocyte subsets and harvested at D7 (Fig. 6a). Besides DCs many resident airway and interstitial macrophages are CD11c+, express the CD11c-DTR transgene, and can be depleted by DTX[28]. However, despite this combinatorial depletion of cell populations, DTX treatment did not reduce granuloma volume or collagen deposition in CD11c-DTR chimeras (Fig. 6b–d). In contrast, DTX-treated CD11b-DTR chimeras developed similarly reduced granuloma volume and fibrosis as non-chimeric CD11b-DTR mice. Moreover, the CD11b/c-DTR doubly-depleted chimeras showed no additional decrease in granuloma volume or fibrosis compared with CD11b-DTR chimeras. These data demonstrate that bone marrow-derived CD11b-DTR sensitive but not CD11c-DTR sensitive leukocytes play a crucial role after antigen priming in maintaining Th2-dependent granuloma formation and fibrosis in the lungs of *S. mansoni* egg-challenged mice.

We therefore compared which lung macrophage subsets were selectively depleted in CD11b − versus CD11c-DTR transgenic mice by a single dose of DTX administered between days 3 and 4 after egg challenge. DTX-treated CD11c-DTR mice lost ~80% of both CD11b− and CD11b+ DCs in the granulomatous lung, but the total number of CD11b+ F4/80+ macrophages did not decrease (Fig. 7a). However, Ly6C expression by the surviving macrophages differed dramatically, with the 1:1 ratio of Ly6C+ to Ly6C− macrophages

present in non-DTX treated mice switching to 1:3 in CD11b-DTR mice and 10:1 in CD11c-DTR mice following DTX treatment (Fig. 7b,c). In CD11b-DTR mice, DTX did not significantly alter the proportion of macrophages expressing MHCII or CD64 and only slightly increased the fraction expressing CD11c in the surviving population; only the loss of Ly6C+ cells was pronounced (Fig. 7b, not shown). By contrast, in DTX-treated CD11c-DTR mice, the percentage of CD11c+ macrophages decreased in both the Ly6C positive and negative subsets, but the number of Ly6C+ macrophages actually increased, while the Ly6C − population was almost entirely lost. Thus, the only macrophage subset whose depletion selectively correlates with the failure to maintain lung inflammation and fibrosis is the Ly6C + population, most likely comprising recently recruited monocytes.

Macrophages regulate chemokine production and recruit effector T cells to the lungs

We also examined if macrophage depletion impaired effector T cell homing to inflamed lungs using an adoptive transfer model. To do this we repeated the day 7 endpoint *S. mansoni* egg-induced lung granuloma model (Fig. 2a), but also pre-activated OT-II transgenic $CD4^+$ T-cells using soluble egg antigen to promote Th2 differentiation, delivered CFSE-labeled effector T cells by IV injection on day 6, and euthanized the animals 24 hours later. As expected, very few but equal numbers of donor cells were recovered from the blood and uninvolved inguinal lymph nodes of control and depleted mice. In contrast, fewer CFSE-labeled T cells homed to the lungs and lung-draining lymph nodes in the DTX-treated mice, suggesting macrophages were important for recruiting T-cells to granulomatous tissues and/or their retention (Fig. 8a).

We therefore screened lung tissue for changes in the expression of chemokines involved in the formation and regulation of *S. mansoni* egg-induced granulomas[29,30]. We identified two chemokines, CCL1 and CCL22, whose diminished expression at both the mRNA and protein levels following depletion might impair Th2 effector cell recruitment (Fig. 8b–c). CCL1 and CCL22 can be produced by IL-4/13-stimulated macrophages, attract $CD4^+$ T-cells, and their neutralization can reduce Th2-mediated lung inflammation[31,32]. However, transcription of chemokines did not globally decrease. CCL2, a known monocyte chemoattractant, was increased at all time points following macrophage depletion, likely explaining why the CD11b+ F4/80+ population in the lung shifted towards a monocyte phenotype after the last dose of DTX. In addition, DTX treatment did not reduce the eosinophil composition of granulomas (Fig. 1b, not shown), and consistent with this we observed little to no change in CCL11, a key eosinophil-attracting chemokine. Together, these data demonstrate that macrophages sustain effector $CD4^+$ Th2 responses in the lungs, at least in part, by producing $CD4^+$ Th2 cell-recruiting chemokines.

CD11b-DTR-sensitive cells remain critical after systemic immunization to drive local type 2 immunity induced by airway allergen

We next investigated whether established type 2 immunity to an airway allergen was similarly reduced by depleting CD11b-DTR-sensitive cells. We employed a commonly used model of HDM-induced allergic lung inflammation and treated sensitized mice with DTX just before and during secondary airway challenge (Fig. 9a). Depletion substantially impaired mucus production by airway epithelial cells (Fig. 9b, d) and reduced the

recruitment of leukocytes, particularly eosinophils, into the lung tissue and airway (Fig. 9e). *Ifng Il13, and Il5* mRNA expression were also reduced in depleted mice as were IL-13-responsive genes including *Clca3*, *Muc5ac*, *Arg1*, *Retnla*, and *Chi3l3* (Fig. 9c).

In contrast, depletion had little to no effect on helper T cells in the lung-draining mediastinal lymph node, with the frequency of cytokine producing $CD4^+$ T cells either remaining unchanged (IL-4, IL-13, IL-17A) or increasing slightly (IFN-γ) (Fig. S7a). In the lungs, the per-cell cytokine response of $CD4^+$ T cells was also unaffected (not shown); however, their total numbers were markedly reduced (Fig. S7b–c). Together with the results of related studies[16,33], our data emphasize that homing of Th2 effector cells into lung can depend critically on signals from monocyte-derived cells recruited in the same time frame.

Macrophage depletion during *Nippostrongylus* infection disrupts type 2 cytokine production and suppresses multiple host defense mechanisms in the lung and intestine

Type 2 immunity can cause pathologies but its natural benefit is to protect against infections by pathogens such as parasitic hookworms. *Nippostrongylus brasiliensis* larvae infect mice through the skin, traverse the lungs, and ultimately reach the small intestine where they lay eggs before being expelled in 8–12 days by the host's Th2 response enhancing smooth muscle contractility and mucus production[12,34]. In addition the type 2 response ameliorates the damage caused by parasites migrating through the lungs[10]. We revisited the question of how macrophages contribute to these processes by treating infected CD11b-DTR mice with DTX as parasites migrate through the lungs (day 4), prior to peak egg production (day 7), and during expulsion (day 10) (Fig. 10a). Macrophage depletion did not affect *N. brasiliensis* from maturing and reaching the intestine by day 7, but did impair expulsion of the parasite at day 10 and increased fecundity throughout the infection (Fig. 10b–e).

Delayed parasite expulsion was not due to skewing towards a type 1 or suppressive immune response as *Ifng* transcript levels did not change and *Il10* was reduced at day 7 following depletion (Fig. 10f). Instead, targeting macrophages substantially impaired the type 2 response in the gut. Although Th2-stimulated mucus genes were only marginally reduced (*Clca3*) or unaffected (*Muc5ac*), we found impaired expression of *Retnla*, *Retnlb*, and *Chi3l3*. In the lung, erythrocytes released into the airways by parasite-induced hemorrhage were inefficiently cleared following depletion (not shown) and *Clca3* or *Muc5ac* failed to increase (Fig. 10g). Our findings match similar studies[10,12], but we additionally observed that depleting macrophages prevented or reduced the induction of *IL5* and *IL13* in both the intestine and lung (Fig. 10f–g). Again, this was a localized defect in type 2 immunity because depletion caused scant decreases in cytokine production by $CD4^+$ Th2 cells in the mesenteric lymph nodes (Fig. S8), suggesting that effector T cells rely on macrophages to guide them into inflamed tissue.

Thus, in three distinct models our results argue that $CD11b^+$ $F4/80^+$ macrophages play an indispensable role in maintaining type 2 immune responses in the lung and gut and that even partially interfering with this function reduces inflammation, fibrosis, and host defense mechanisms by disrupting the recruitment of IL-13-producing $CD4^+$ T cells.

Discussion

Macrophages are phagocytic cells that detect, engulf, and destroy microbes, yet this function is only one of the many important roles they play in the immune response. In addition to aiding in host defence, macrophages regulate tissue development, help maintain and restore organ function, regulate metabolic pathways, dispose of dying cells and cellular debris, and promote or resolve inflammation[3,9,35–39]. One reason macrophages are capable of playing such diverse roles is that their activation state is not fixed, enabling them to adapt and alter their function in response to changes in the local environment. This inherent plasticity is readily apparent in tissue repair and fibrosis, where macrophages are thought to play both pro- and anti-fibrotic roles at various stages of wound healing responses[37,39,40].

Here we present evidence that macrophages must continue to recruit, and perhaps retain, effector CD4 T cells in the lung or type 2 immune responses will begin to abate. We believe this is a novel and important discovery because it demonstrates mechanistically how even strong and fully developed IL-13-dependent fibrosis and other type 2-driven inflammatory pathologies could be disrupted by transiently targeting one type of leukocyte. In this study, using three distinct Th2 models and CD11b-DTR and CD11c-DTR transgenic mice, we showed that CD11b+ F4/80+ macrophages but not CD11c+ DCs are critical to the maintenance of type 2-driven tissue inflammation and lung fibrosis but are less critical to the maintenance of type-2 immunity in secondary lymphoid organs. The *S. mansoni* egg-induced granuloma model creates an extremely robust type 2 inflammatory response that develops synchronously and in distinct stages in the lung, with >50% of all CD4+ T cells infiltrating the lung capable of producing IL-13. In antigen-primed mice, this model of IL-13-dependent fibrosis is robust enough to more than double the collagen content of the lung. We designed our experiments to compare the consequences of depleting macrophages during the formative, maintenance, and resolution stages of IL-13-driven inflammation and fibrosis. Surprisingly, even when macrophages were depleted after granulomas had formed and fibrosis was established, we found a rapid, large, and broad reduction in the type 2 immune response in the lung but not in the draining lymph node, with no evidence that macrophages were switching their phenotype in aggregate from inducers to resolvers of inflammation and fibrosis. These results demonstrate that macrophages are required to maintain IL-13-dependent fibrogenesis in the lung even during the stage when inflammation is clearing.

Previous studies have examined the roles of different leukocyte populations at the onset of immune activation and lung pathology using the CD11b-DTR, CD11c-DTR, and clodronate-loaded liposome depletion technologies, as well as in CCR2-deficient mice to impair monocyte mobilization[10,16–18,28,33,41]. All such data, including the results we present here, warrant cautious interpretation since macrophage depletion by any of these methods is incomplete and varies by location, duration, and cellular subset. Overall, these studies concluded that monocyte-derived populations play critical roles at the start of inflammatory responses. However, these tissue-infiltrating monocytes exhibited phenotypes and functions that made it difficult to neatly categorize them as “macrophages”, “monocytes”, or “dendritic cells”. The CD11c-DTR and clodronate methods have been reported to target a wider range of cell populations in inflamed lungs than CD11b-DTR mice. In our studies

DTX treatment depleted approximately half of all the CD11b-DTR F4/80+ macrophages in the inflamed lung, and primarily the Ly6C+ subset, without ablating eosinophils, neutrophils, or F4/80− dendritic cells. In our experimental system, we found DTX-treated CD11c-DTR mice lost CD11b− DCs, CD11b+ DCs, and CD11c+ Ly6C− but not Ly6C+ macrophages. Our results support investigations of HDM-induced lung inflammation, which showed chemokine secretion and antigen presenting by “monocyte-derived dendritic cells” in the lung are crucial to the initiation of type 2 lung inflammation[33,42]. In our study, we identified that a CD11b-DTR-sensitive F4/80+ Ly6C+ lung macrophage population, likely similarly derived from monocytes, is critical to maintain inflammatory type 2 immune responses. We did not design this study to discriminate between macrophages of different origins. However, the number of macrophages, disproportionate depletion of the Ly6C+ subset, and pattern of CCL2 expression most likely indicate large-scale, CD11b-DTR-sensitive monocyte immigration into the lungs, as was recently described in the liver of *S. mansoni* infected mice[43]. By contrast, the CD11b(low) CD11c+ alveolar subset of resident macrophages is reported to resist depletion during challenge in CD11b-DTR mice[16–18], suggesting that lung inflammation and fibrosis in our experiments crucially depends on monocyte-derived macrophages.

Although macrophages were critical to the maintenance of established type 2 responses in the affected tissues, there was no obvious diminution in the differentiation and activation of CD4+ Th2 cells in the draining lymph nodes. Such compartmentalization adds to the preponderance of evidence that dendritic cells, but not monocyte-derived or resident macrophages, initiate T cell responses in lymph nodes. In some cases monocytes also function and/or differentiate into DCs[33,44], but such a role is dispensable outside the lung and after antigen priming in our experiments. Conversely, CD11c-DTR-dependent depletion beginning 3 days after challenging antigen-primed mice did not reduce inflammation or fibrosis in the lung, and combining CD11c-DTR depletion had no additional impact over CD11b-DTR alone in bone marrow chimeras. We also found CD11c-DTR transgenic mice lost ~80% of both CD11b− and CD11b+ DCs, in the granulomatous lung after 1 dose of DTX. Therefore, the dendritic cells depleted in this system are not required after initiation to maintain established type 2 responses in the lung, further emphasizing the important localized role played by $CD11b^+$ $F4/80^+$ Ly6C+ macrophages.

Why macrophages are critical to the maintenance of type 2 immunity was difficult to pin down because macrophages produce a variety of growth factors, cytokines, and chemokines that can diversely influence the maintenance of adaptive immune responses. Since type 2 immunity was reduced in the tissues but not in the draining lymph nodes of depleted mice, we tested T cell homing to the inflamed lungs. Strikingly, we showed that depleting macrophages reduced the number of pre-activated and transferred Th2 cells in the lungs and lung-draining mediastinal lymph nodes. Since effector T cells do not generally home directly to lymph nodes, the combined decrease of donor cells in both locations 1 day after transfer likely results from impaired recruitment from the bloodstream to the lungs followed by drainage from lung to lymph node. Our use of ovalbumin-specific T cells likely favors emigration from the lungs because these cells cannot locate their cognate antigen, but also adds evidence discriminating between weaker recruitment and a lower probability of locating and being retained in contact with an antigen-presenting cell. We therefore interpret

our results to mean that macrophage depletion impaired the recruitment, and/or retention, of $CD4^+$ effector T cells to the lungs of *S. mansoni* egg-challenged mice.

Furthermore, chemokines CCL1 and CCL22, which are known $CD4^+$ Th2 cell chemoattractants produced by IL-4/13-stimulated macrophages, were markedly decreased in the lungs following DTX treatment, providing at least one explanation for the decreased type 2 responses in the lung and gut. We also found correlating evidence that the reduced number of effector T cells still homing to the lungs after depletion were additionally impaired because of decreased antigen presentation. CD4 T cells recovered from the lungs, but not draining lymph nodes, of DTX-treated CD11b-DTR mice produced less cytokines both as a percent of the population and per cell. In parallel, DTX treatment shifted the predominant phenotype of macrophages on day 7 from MHCII+ CD11c+ Ly6C− to MHCII− CD11c− Ly6C+. This shift suggests that most of the monocytes would otherwise develop into functioning antigen-presenting cells and the depleted populations are replaced by cells yet to acquire the same functions. However, full-scale lung inflammation and fibrosis developed despite targeting CD11c+ leukocytes.

In our experiments, Th17 cells outside the lungs are scarcely affected by macrophage depletion (Fig. 5a, S5, S7a, S8). But, as for Th2 cells, loss of macrophages decreased the IL-17A+ CD4 T cell population within the lung primarily by reducing the total number of T cells (Fig. 5b–d, S7c). Recruitment of both Th2 and Th17 cells to the granulomatous lungs may therefore depend on macrophages. However, DTX treatment increased neutrophil inflammation without causing lung hemorrahage, necrosis, and the characteristic pathologies of severely disabled Th2 and/or exacerbated Th17 responses [10,45,46]. This suggests either another source of IL-17A increases or that neutrophils are recruited by an IL-17A-independent mechanism, but also that this influx of neutrophils does not damage the lung and perhaps aids in clearing extracellular matrix. A likely beneficial effect from neutrophils in IL-13-dependent fibrosis would contrast with their presumed role as a pro-fibrotic effector in other models, such as IL-1- and TGFβ-dependent bleomycin-induced lung injury [47].

Previous studies using clodronate liposomes to deplete phagocytic cells suggested that alternatively activated macrophages, which predominate during infection with the nematode *H. polygyrus*, are directly involved in parasite expulsion from the gut[10]. Although the exact anti-parasite mechanism was not identified, the authors hypothesised that macrophages could directly impair parasite mobility and fitness as suggested in a study by Bieren *et al*[48]. Surprisingly, clodronate treatment caused no reduction in IL-4 or IL-13 gene expression in the mesenteric lymph nodes or proximal small intestines, suggesting unimpaired T cell activation and homing despite phagocyte depletion. In contrast, in our studies using CD11b-DTR mice we observed a marked reduction in type 2 tissue cytokine expression in all three Th2 models examined. In the case of *N. brasiliensis* infection, this resulted in a weaker induction of several mechanisms implicated in anti-nematode immunity, including mucin production and *Retnlb* expression[10,12]. Thus, while macrophages also participate directly in anti-nematode immunity, our findings suggest that they are critically and more broadly involved in the maintenance of the entire type 2 host defence and tissue repair programs in the lung and gut.

In conclusion, our studies from three different Th2 models demonstrate that macrophages contribute to the maintenance of type 2 immune responses in the lung and gut. They may play this role after the initiation of an immune response by producing chemokines that recruit effector T cells to inflamed tissue and by presenting antigens to reactivate the arriving T cells. Importantly, this role for macrophages appears to be needed continuously by ongoing type 2 immune reactions in the lung and gut. Thus, therapies designed to transiently but specifically target the migration, survival, or activation of macrophages could emerge as viable treatments for a host of important diseases that are defined by the persistent overproduction of type 2-associated cytokines and chronic inflammation.

Methods

Materials, mice, and macrophage depletion

All reagents were from Sigma Aldrich unless stated otherwise. All experiments were performed at the National Institutes of Health using mice bred and housed under specific pathogen-free conditions in an American Association for the Accreditation of Laboratory Animal Care approved facility under Animal Study Proposal LPD-16E. The NIAID animal care and use committee approved all experimental procedures.

CD11b-DTR (FVB-Tg(ITGAM-DTR/EGFP)34Lan/J) and CD11c-DTR (B6.FVB-Tg(Itgax-DTR/EGFP)57Lan/J) transgenic mice were obtained from The Jackson Laboratory. CD11c-DTR mice were crossed with CD45.1 congenic mice (B6.SJL-Ptprc^{a} Pepc^{b}/BoyJ). Homozygous colonies were maintained on a C57Bl/6 background, and either crossed with WT mice (Taconic) to produce hemizygous transgenic mice for experiments or intercrossed to generate doubly hemizygous transgenic mice (CD11b/c-DTR).

Diphtheria toxin (DTX, Sigma) was reconstituted to 2mg/ml in sterile water and then diluted to 2.5μg/ml in sterile saline. Mice were randomly assigned to control and experimental groups. Experimental mice were injected via the intraperitoneal route (IP) with DTX (25ng/g) as indicated for each experimental model.

Schistosome egg-induced lung granulomas

Schistosoma mansoni eggs were provided by the Biomedical Research Institute (Rockville, MD). For the secondary lung granuloma model, mice were primed with IP injection of 5,000 eggs in PBS on D-14 and injected intravenously (IV) with 5,000 live eggs in PBS at D0 to induce lung granulomas. Half of the mice were treated with DTX (25ng/g) when indicated (Fig. 2a). Mice were euthanized by pentobarbital overdose plus heparin on D4, D7 or D14. For the primary lung granuloma model, mice were treated as above without IP priming. For histological analyses, matched lung lobes were washed with PBS, inflated with Bouin's fixative, and stained with Masson's Trichrome. Granuloma volume was determined by an experienced pathologist blinded to groups scoring 5–30 granulomas per mouse. For assessment of fibrosis, matched lung lobes were weighed and digested with 2ml of 6N HCl to measure the quantity of hydroxyproline[49], or sections were stained with picrosirius red to evaluate collagen distribution. Matched samples of lung tissue for quantitative PCR were collected and processed as below.

House Dust Mite treatment

Mice were primed by IP injection of 200μg of house dust mite (HDM, Greer) in sterile saline on D0 and D7. Primed mice were challenged by intratracheal instillation of 50μg of HDM in 30μl of sterile saline (or 30μl of sterile saline as a control) on D14 and D16. Half the mice were treated with DTX (25ng/g) at D13 and D15 (Fig. 9a). Mice were euthanized by pentobarbital overdose plus heparin 24 h after the last HDM challenge and their tracheas cannulated with an Insyte venous catheter (BD). Bronchoalveolar lavage (BAL) was performed with ice cold PBS supplemented with 5mM EDTA. Percentage of eosinophils was determined using cytospin preparations stained with Diff-Quick (Boehringer) by evaluating >200 cells/slide. For histological analyses of epithelial mucus, lung lobes were inflated with Bouin's fixative, stained with Alcian Blue-Periodic Acid Schiff (AB-PAS) and scored by an experienced pathologist blinded to groups. Matched samples of lung tissue for quantitative PCR were collected and processed as below.

Nippostrongylus infection

Preparation and the subcutaneous inoculation of mice with 500 infective third-stage *Nippostrongylus brasiliensis* larvae (L3) were performed as described[34]. *N. brasiliensis* eggs were initially provided by Dr. Joe Urban (USDA, Beltsville, MD). Half the mice were treated with DTX (25ng/g) when indicated (Fig. 10a). Mice were euthanized by pentobarbital overdose plus heparin on D4 (for lung studies) and D7 or D10 (for gut). Longitudinal egg counts in fecal pellets were performed daily from D6 to D10. Endpoint intestinal worm counts and fecal egg counts were measured on D7 and D10. Matched samples of lung (D4) and gut (D7 & D10) tissue for quantitative PCR were collected and processed as below.

Quantitative PCR

Tissue samples were mechanically homogenized in Trizol using beads and a Precellys24 (Bertin Technologies). RNA was extracted with chloroform, isolated with a MagMAX total RNA isolation kit, and reverse transcribed with Superscript II. Gene expression was measured by quantitative PCR amplification of cDNA using SYBR Green on an ABI Prism 7900HT Sequence Detection System (all from Life Technologies) and normalized to RPLP2. Real time PCR data was analyzed using the comparative Ct method using SAGE software (https://sage.niaid.nih.gov). All experiments used intron-spanning primers validated by dissociation curves, see table 1.

Chemokine ELISA

Snap frozen lung lobes were homogenized in RIPA lysis buffer (Santa Cruz Biotechnology) using a Precellys24 (Bertin Technologies). Protein concentration of the clarified lysates were measured by absorbance at 280 nm using Nanodrop. Concentration of CCL1, CCL2 and CCL22 were measured in the lysate using respective ELISA kits (RnD systems) as per manufacturer's protocol.

Lung leukocyte isolation

Lung leukocytes were isolated by digesting PBS perfused matched lung lobes after mincing in collagenase IV (100U/ml in RPMI) for 60 min rocking at 37°C, crushing through a 100μM cell strainer, underlaying with isotonic 36% Percoll (GE Healthcare) and centrifuging for 20 mins at 350xg. Erythrocytes were eliminated using ACK lysis buffer (Quality Biological). Lung leukocyte numbers were determined using Trypan blue and a Cellometer Auto T4 (Nexcelom) or hemocytometer.

T cell restimulation and flow cytometry

To assess intracellular cytokines, leukocytes were stimulated for 4 hrs with phorbol 12-myristate 13-acetate (10 ng/ml), ionomycin (1 μg/ml) and brefeldin A (10 μg/ml). Cells were washed, fixed in 2% paraformaldehyde, permeabilized with 0.5% saponin buffer and stained with antibodies specific for CD4 (Biolegend – RM4-5), IFN-γ (eBioscience – XMG1.2), IL-4 (eBioscience – 11B11), IL-13 (eBioscience – eBio13A) and IL-17A (Biolegend – TC11-18H10.1). To assess cell populations and macrophage depletion, leukocytes isolated from lung tissue or 72 hrs thioglycollate elicited peritoneal cells (3% w/v) were labelled with a viability dye (Invitrogen – LIVE/DEAD Blue or Aqua), pre-incubated in 2% normal rat serum plus unlabelled anti-CD16/32 antibody (eBioscience – 93), and stained with combinations of antibodies specific for: CD11b (Biolegend – M1/70), CD11c (BD – HL3), CD45 (Biolegend - 30-F11), CD64 (Biolegend – X54-5/7.1), F4/80 (Biolegend – BM8), Gr-1 (Biolegend – RB6-8C5), Ly6C (Biolegend – HK1.4), Ly6G (BD – 1A8), MHC class II I-Ab (BD – AF6-120.1) or I-A/E (Biolegend M5/114.15.2), Siglec-F (BD – E50-2440), and TCRβ (eBioscience – H57-597). Flow cytometry was performed using a FACSCanto II or LSRII (BD Biosciences) and data were analyzed using FlowJo (Tree Star).

T cell adoptive transfer

Antigen-presenting cells (APCs) were prepared from naïve C57BL/6 or CD11b-DTR mice. Spleens were digested in collagenase (100U/ml in RPMI) for 60 min rocking at 37°C, mechanically dispersed to generate single cell suspensions, and treated with ACK lysis buffer to eliminate erythrocytes. Spleen plus peripheral and mesenteric lymph nodes of ovalbumin-specific OT-II TCR transgenic donor mice were processed similarly, labelled with biotinylated anti-CD4 antibody (eBioscience – GK1.5), then enriched for CD4+ T cells by positive selection with MACS LS columns and streptavidin or anti-biotin beads (Miltenyi Biotec). APCs were irradiated with 3,300 rads. To activate OT-II cells *in vitro*, 10 irradiated APCs per CD4+ cell were cultured at 37°C in RPMI plus 1 ug/mL ovalbumin 323–339 peptide and 1 or 20 ug/mL soluble egg antigen. Culture media was supplemented with 10U/mL rhIL-2 (NCI repository). Recipient mice (CD11b-DTR) were primed by IP injection of 5,000 *S. mansoni* eggs in PBS on D-14 and injected IV with 5,000 live eggs in PBS at D0 to induce lung granulomas. Half the mice were treated with DTX (25ng/g) at D3, D4 and D5. On D6 CD4+ T cells (4×10^6) labelled with CFSE (5μM for 10mins at room temperature) were injected IV in 300 μl of PBS to recipient mice. Mice were euthanized by pentobarbital overdose plus heparin 24 hours later. The number of CFSE labelled CD4+ cells in blood, lung, inguinal lymph nodes and mediastinal lymph nodes was assessed by flow cytometry.

Bone marrow chimeras

Bone marrow was harvested from the femur and tibia of C57Bl/6, CD11b-DTR, CD11c-DTR and CD11b/c-DTR mice, washed, filtered, resuspended in PBS and injected IV (4×10^6 cells) into lethally irradiated (900 rads) C57Bl/6 recipient mice. Mice were provided antibiotic-containing water (Trimethoprim-sulfa) for 4 weeks and used for experiments 7 weeks after reconstitution.

Statistical analyses

All data were analyzed with Prism (GraphPad Software). Data were considered statistically significant for *P* values less than 0.05, obtained with a two-tailed *t*-test or Mann-Whitney U test. Differences are noted as * $p<0.05$, ** $p<0.01$, *** $p<0.001$, or ns (not significant).

Supplementary Material

Refer to Web version on PubMed Central for supplementary material.

Acknowledgments

We would like to express our sincere appreciation and thanks to all of our colleagues, past and present, for their guidance and support. LAB is supported by a Marie Curie international outgoing fellowship from the European Union Framework Programme 7. TAW is supported by the Intramural Research Program of the NIH/NIAID.

References

1. Holgate ST. Innate and adaptive immune responses in asthma. Nature medicine. 2012; 18:673–683. DOI: 10.1038/nm.2731
2. Bamias G, Kaltsa G, Ladas SD. Cytokines in the pathogenesis of ulcerative colitis. Discovery medicine. 2011; 11:459–467. [PubMed: 21616044]
3. Anthony RM, Rutitzky LI, Urban JF Jr, Stadecker MJ, Gause WC. Protective immune mechanisms in helminth infection. Nature reviews. Immunology. 2007; 7:975–987. DOI: 10.1038/nri2199
4. Jakubzick C, et al. Minimal differentiation of classical monocytes as they survey steady-state tissues and transport antigen to lymph nodes. Immunity. 2013; 39:599–610. DOI: 10.1016/j.immuni.2013.08.007 [PubMed: 24012416]
5. Hashimoto D, et al. Tissue-resident macrophages self-maintain locally throughout adult life with minimal contribution from circulating monocytes. Immunity. 2013; 38:792–804. DOI: 10.1016/j.immuni.2013.04.004 [PubMed: 23601688]
6. Guilliams M, et al. Alveolar macrophages develop from fetal monocytes that differentiate into long-lived cells in the first week of life via GM-CSF. The Journal of experimental medicine. 2013; 210:1977–1992. DOI: 10.1084/jem.20131199 [PubMed: 24043763]
7. Geissmann F, et al. Development of monocytes, macrophages, and dendritic cells. Science. 2010; 327:656–661. DOI: 10.1126/science.1178331 [PubMed: 20133564]
8. Jenkins SJ, et al. Local macrophage proliferation, rather than recruitment from the blood, is a signature of TH2 inflammation. Science. 2011; 332:1284–1288. DOI: 10.1126/science.1204351 [PubMed: 21566158]
9. Pittet MJ, Nahrendorf M, Swirski FK. The journey from stem cell to macrophage. Annals of the New York Academy of Sciences. 2014; 1319:1–18. DOI: 10.1111/nyas.12393 [PubMed: 24673186]
10. Chen F, et al. An essential role for TH2-type responses in limiting acute tissue damage during experimental helminth infection. Nature medicine. 2012; 18:260–266. DOI: 10.1038/nm.2628
11. Perrigoue JG, et al. MHC class II-dependent basophil-CD4+ T cell interactions promote T(H)2 cytokine-dependent immunity. Nature immunology. 2009; 10:697–705. DOI: 10.1038/ni.1740 [PubMed: 19465906]

12. Zhao A, et al. Th2 cytokine-induced alterations in intestinal smooth muscle function depend on alternatively activated macrophages. Gastroenterology. 2008; 135:217–225. e211. DOI: 10.1053/j.gastro.2008.03.077 [PubMed: 18471439]
13. Duffield JS, et al. Selective depletion of macrophages reveals distinct, opposing roles during liver injury and repair. The Journal of clinical investigation. 2005; 115:56–65. DOI: 10.1172/JCI22675 [PubMed: 15630444]
14. Cailhier JF, et al. Conditional macrophage ablation demonstrates that resident macrophages initiate acute peritoneal inflammation. Journal of immunology. 2005; 174:2336–2342.
15. Lin SL, Castano AP, Nowlin BT, Lupher ML Jr, Duffield JS. Bone marrow Ly6Chigh monocytes are selectively recruited to injured kidney and differentiate into functionally distinct populations. Journal of immunology. 2009; 183:6733–6743. DOI: 10.4049/jimmunol.0901473
16. Medoff BD, et al. CD11b+ myeloid cells are the key mediators of Th2 cell homing into the airway in allergic inflammation. Journal of immunology. 2009; 182:623–635.
17. Dhaliwal K, et al. Monocytes control second-phase neutrophil emigration in established lipopolysaccharide-induced murine lung injury. American journal of respiratory and critical care medicine. 2012; 186:514–524. DOI: 10.1164/rccm.201112-2132OC [PubMed: 22822022]
18. Crapster-Pregont M, Yeo J, Sanchez RL, Kuperman DA. Dendritic cells and alveolar macrophages mediate IL-13-induced airway inflammation and chemokine production. The Journal of allergy and clinical immunology. 2012; 129:1621–1627. e1623. DOI: 10.1016/j.jaci.2012.01.052 [PubMed: 22365581]
19. Lee S, et al. Distinct macrophage phenotypes contribute to kidney injury and repair. Journal of the American Society of Nephrology: JASN. 2011; 22:317–326. DOI: 10.1681/ASN.2009060615 [PubMed: 21289217]
20. Wynn TA, Eltoum I, Oswald IP, Cheever AW, Sher A. Endogenous interleukin 12 (IL-12) regulates granuloma formation induced by eggs of Schistosoma mansoni and exogenous IL-12 both inhibits and prophylactically immunizes against egg pathology. The Journal of experimental medicine. 1994; 179:1551–1561. [PubMed: 7909326]
21. Lewis, F. Schistosomiasis. In: Coligan, John E., et al., editors. Current protocols in immunology. Vol. Chapter 19. 2001. p. 11
22. Hesse M, et al. The pathogenesis of schistosomiasis is controlled by cooperating IL-10-producing innate effector and regulatory T cells. Journal of immunology. 2004; 172:3157–3166.
23. Hesse M, Cheever AW, Jankovic D, Wynn TA. NOS-2 mediates the protective anti-inflammatory and antifibrotic effects of the Th1-inducing adjuvant, IL-12, in a Th2 model of granulomatous disease. Am J Pathol. 2000; 157:945–955. DOI: 10.1016/S0002-9440(10)64607-X [PubMed: 10980133]
24. Chiaramonte MG, Donaldson DD, Cheever AW, Wynn TA. An IL-13 inhibitor blocks the development of hepatic fibrosis during a T-helper type 2-dominated inflammatory response. Journal of Clinical Investigation. 1999; 104:777–785. DOI: 10.1172/Jci7325 [PubMed: 10491413]
25. Chiaramonte MG, Cheever AW, Malley JD, Donaldson DD, Wynn TA. Studies of murine schistosomiasis reveal interleukin-13 blockade as a treatment for established and progressive liver fibrosis. Hepatology. 2001; 34:273–282. DOI: 10.1053/jhep.2001.26376 [PubMed: 11481612]
26. Fallon PG, Richardson EJ, McKenzie GJ, McKenzie ANJ. Schistosome infection of transgenic mice defines distinct and contrasting pathogenic roles for IL-4 and IL-13: is a profibrotic agent. Journal of immunology. 2000; 164:2585–2591.
27. Jung S, et al. In vivo depletion of CD11c+ dendritic cells abrogates priming of CD8+ T cells by exogenous cell-associated antigens. Immunity. 2002; 17:211–220. [PubMed: 12196292]
28. Padilla J, et al. IL-13 regulates the immune response to inhaled antigens. Journal of immunology. 2005; 174:8097–8105.
29. Park MK, et al. Patterns of chemokine expression in models of Schistosoma mansoni inflammation and infection reveal relationships between type 1 and type 2 responses and chemokines in vivo. Infection and immunity. 2001; 69:6755–6768. DOI: 10.1128/IAI.69.11.6755-6768.2001 [PubMed: 11598048]

30. Souza PR, Souza AL, Negrao-Correa D, Teixeira AL, Teixeira MM. The role of chemokines in controlling granulomatous inflammation in Schistosoma mansoni infection. Acta tropica. 2008; 108:135–138. DOI: 10.1016/j.actatropica.2008.04.016 [PubMed: 18514159]

31. Mantovani A, et al. The chemokine system in diverse forms of macrophage activation and polarization. Trends in immunology. 2004; 25:677–686. DOI: 10.1016/j.it.2004.09.015 [PubMed: 15530839]

32. Jakubzick C, et al. Role of CCR4 ligands, CCL17 and CCL22, during Schistosoma mansoni egg-induced pulmonary granuloma formation in mice. Am J Pathol. 2004; 165:1211–1221. DOI: 10.1016/S0002-9440(10)63381-0 [PubMed: 15466387]

33. Plantinga M, et al. Conventional and monocyte-derived CD11b(+) dendritic cells initiate and maintain T helper 2 cell-mediated immunity to house dust mite allergen. Immunity. 2013; 38:322–335. DOI: 10.1016/j.immuni.2012.10.016 [PubMed: 23352232]

34. Camberis, M.; Le Gros, G.; Urban, J, Jr. Animal model of Nippostrongylus brasiliensis and Heligmosomoides polygyrus. In: Coligan, John E., et al., editors. Current protocols in immunology. Vol. Chapter 19. 2003. p. 12

35. Allen JE, Wynn TA. Evolution of Th2 immunity: a rapid repair response to tissue destructive pathogens. PLoS pathogens. 2011; 7:e1002003. [PubMed: 21589896]

36. Wynn TA, Chawla A, Pollard JW. Macrophage biology in development, homeostasis and disease. Nature. 2013; 496:445–455. DOI: 10.1038/nature12034 [PubMed: 23619691]

37. Barron L, Wynn TA. Fibrosis is regulated by Th2 and Th17 responses and by dynamic interactions between fibroblasts and macrophages. American journal of physiology. Gastrointestinal and liver physiology. 2011; 300:G723–728. DOI: 10.1152/ajpgi.00414.2010 [PubMed: 21292997]

38. Duffield JS, Lupher M, Thannickal VJ, Wynn TA. Host responses in tissue repair and fibrosis. Annual review of pathology. 2013; 8:241–276. DOI: 10.1146/annurev-pathol-020712-163930

39. Murray PJ, Wynn TA. Protective and pathogenic functions of macrophage subsets. Nature reviews. Immunology. 2011; 11:723–737. DOI: 10.1038/nri3073

40. Wynn TA, Barron L. Macrophages: master regulators of inflammation and fibrosis. Seminars in liver disease. 2010; 30:245–257. DOI: 10.1055/s-0030-1255354 [PubMed: 20665377]

41. van Rijt LS, et al. In vivo depletion of lung CD11c+ dendritic cells during allergen challenge abrogates the characteristic features of asthma. The Journal of experimental medicine. 2005; 201:981–991. DOI: 10.1084/jem.20042311 [PubMed: 15781587]

42. Hammad H, et al. Inflammatory dendritic cells--not basophils--are necessary and sufficient for induction of Th2 immunity to inhaled house dust mite allergen. The Journal of experimental medicine. 2010; 207:2097–2111. DOI: 10.1084/jem.20101563 [PubMed: 20819925]

43. Girgis NM, et al. Ly6Chigh Monocytes Become Alternatively Activated Macrophages in Schistosome Granulomas with Help from CD4+ Cells. PLoS pathogens. 2014; 10:e1004080. [PubMed: 24967715]

44. Jakubzick C, et al. Blood monocyte subsets differentially give rise to CD103+ and CD103− pulmonary dendritic cell populations. Journal of immunology. 2008; 180:3019–3027.

45. Barron L, Wynn TA. Macrophage activation governs schistosomiasis-induced inflammation and fibrosis. European journal of immunology. 2011; 41:2509–2514. DOI: 10.1002/eji.201141869 [PubMed: 21952807]

46. Ramalingam TR, et al. Unique functions of the type II interleukin 4 receptor identified in mice lacking the interleukin 13 receptor alpha1 chain. Nature immunology. 2008; 9:25–33. DOI: 10.1038/ni1544 [PubMed: 18066066]

47. Wilson MS, et al. Bleomycin and IL-1beta-mediated pulmonary fibrosis is IL-17A dependent. The Journal of experimental medicine. 2010; 207:535–552. DOI: 10.1084/jem.20092121 [PubMed: 20176803]

48. Bieren JEV, et al. Antibodies Trap Tissue Migrating Helminth Larvae and Prevent Tissue Damage by Driving IL-4R alpha-Independent Alternative Differentiation of Macrophages. PLoS pathogens. 2013; 9:ARTN e1003771.

49. Wynn, TA., et al. Quantitative assessment of macrophage functions in repair and fibrosis. In: Coligan, John E., et al., editors. Current protocols in immunology. Vol. Chapter 14. 2011. p. 22

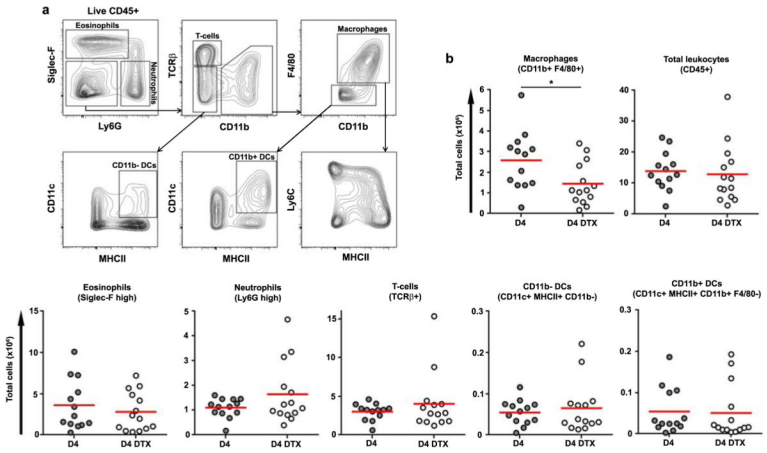

Figure 1. DTX treatment of primed and challenged CD11b-DTR mice causes direct, partial, and selective depletion of CD11b+ F4/80+ macrophages within the granulomatous lung

CD11b-DTR egg primed and challenged mice were treated with DTX (n=14) or left untreated (n=13) on D3 and harvested on D4. Lung leukocytes were analysed by flow cytometry to identify directly depleted cell types. **(a)** Representative flow cytometry plots of untreated D4 lung leukocytes (live CD45+) showing the gating strategy used to distinguish eosinophils (Siglec-F+ Ly6G-/low), neutrophils (Siglec-F− Ly6Ghigh), T cells (TCRβ+), macrophages (F4/80+ CD11b+) as well as CD11b− and CD11b+ DCs (CD11c+ MHCII+ F4/80−). DTX treatment **(b)** directly reduced the number of CD11b+ F4/80+ macrophages but not other leukocytes in the lung. Statistical significance was calculated using unpaired two-tailed Student's *t* test. * p<0.05, ** p<0.01, *** p<0.001. Results represent three independent experiments.

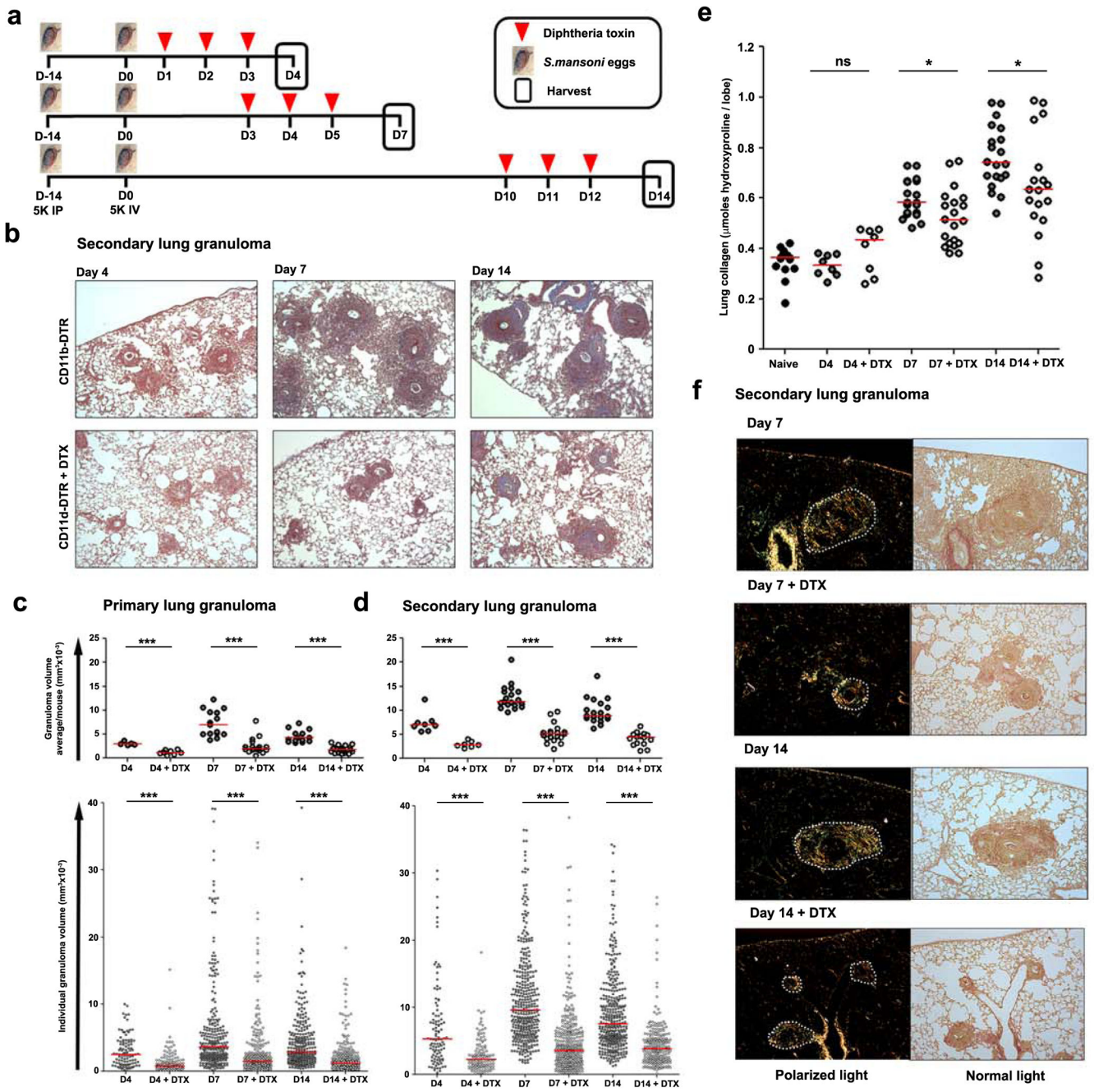

Figure 2. Macrophages are critical promoters of both the local induction and maintenance of type 2-dependent lung fibrosis

(a) CD11b-DTR mice were primed by IP injection of 5,000 *S. mansoni* eggs on D-14 and then challenged by a single IV injection of 5,000 live eggs on D0. Mice were harvested at the initiation (D4), peak (D7) or resolution (D14) stages of lung granuloma formation. Half of the mice were treated with DTX (25ng/g) when indicated. **(b)** Representative images showing inflammation and collagen (blue) in Masson's Trichrome stained lung tissue from primed and challenged (CD11b-DTR) (Primary lung granuloma D4 n=5; D7 n=15; D10 n=15; Secondary lung granuloma D4 n=8; D7 n=19; D10 n=19), and primed, challenged,

and DTX treated (CD11b-DTR + DTX) (Primary lung granuloma D4 n=8; D7 n=18; D10 n=19; Secondary lung granuloma D4 n=7; D7 n=19; D10 n=15) CD11b-DTR mice. Volumes of **(c)** primary lung granulomas (intravenous challenge without priming) and **(d)** secondary lung granulomas (intraperitoneal primed, intravenous challenged) were scored by a pathologist blinded to groups and data presented as average granuloma volume/mouse (top panel) and individual granuloma volume (bottom panel). DTX treatment reduced both primary and secondary lung granuloma volumes at all-time points assessed. **(e)** Change in collagen deposition in egg primed and challenged CD11b-DTR mice with or without DTX treatment was compared by measuring hydroxyproline content of lung tissue. **(f)** Collagen was visualized by picrosirius red staining of lung tissue exposed to polarized and normal transmitted light. Dotted lines outline granulomas. DTX treatment reduced lung collagen at D7 and 14. Data are presented as median and statistical significance calculated using Mann-Whitney U test. * $p<0.05$, *** $p<0.001$. Results represent two independent experiments.

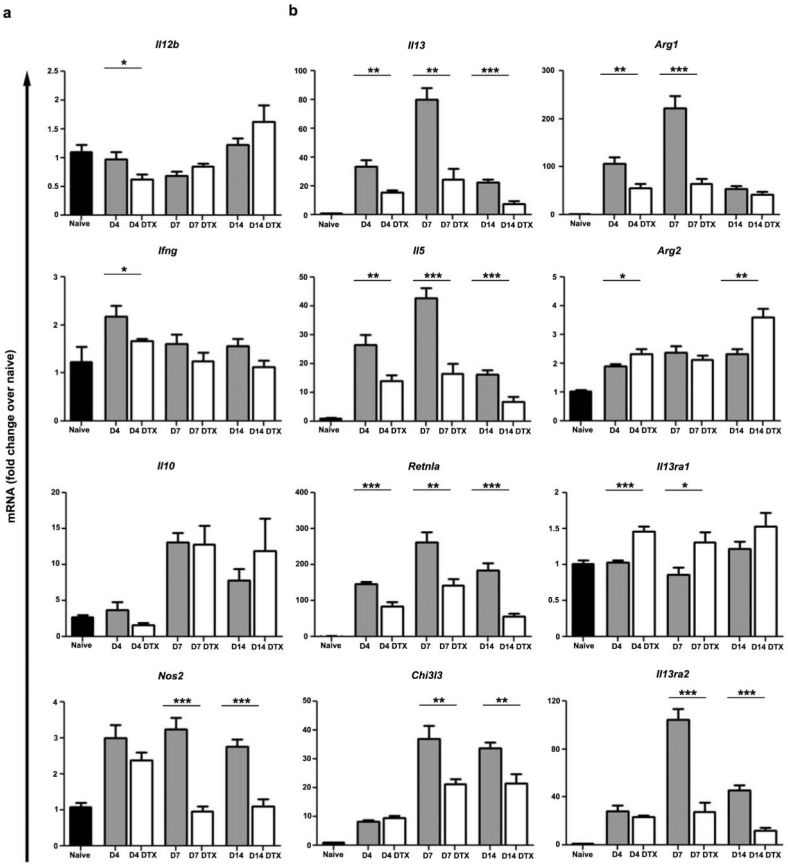

Figure 3. Type 2 immunity in the granulomatous lung is dependent on macrophages

Relative quantitative gene expression in lung tissue of naïve (n=13), egg primed and challenged (D4 n=8; D7 n=9, D10 n=10), and primed, challenged, and DTX treated (D4 n=8; D7 n=10, D10 n=9) CD11b-DTR mice. Results were normalized to RPLP2 and scaled to naïve mice. All Th2-induced genes were more weakly induced by egg challenge following DTX treatment. Data are presented as mean ± s.e.m. Statistical significance was calculated using unpaired two-tailed Student's *t* test. * $p<0.05$, ** $p<0.01$, *** $p<0.001$. Results represent two independent experiments.

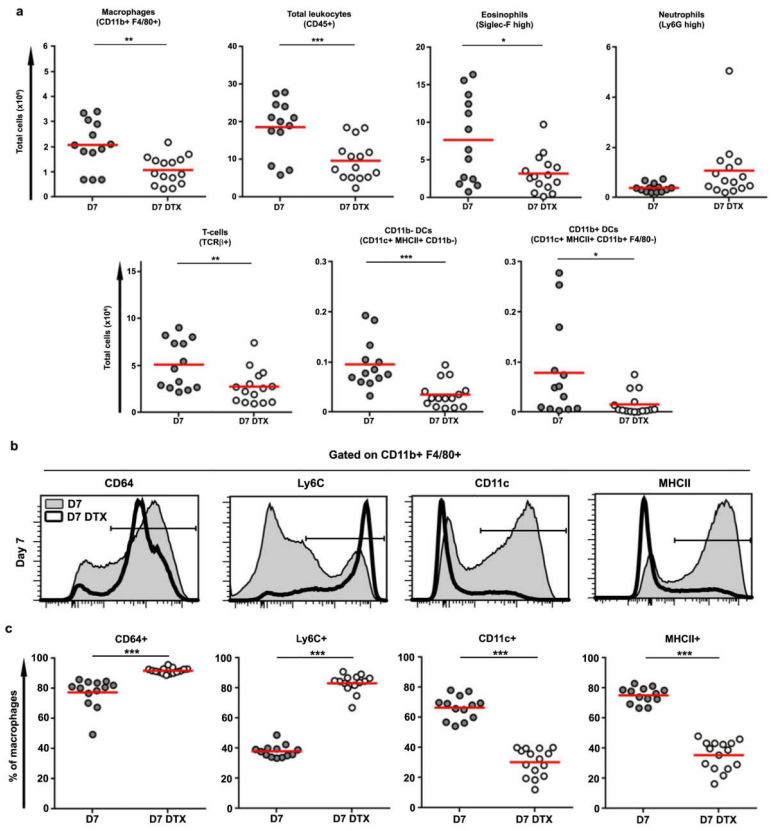

Figure 4. Direct depletion of macrophages in the granulomatous lung indirectly reduces inflammation and leads to their replacement by cells with a monocyte phenotype

CD11b-DTR egg primed and challenged mice were treated with DTX (n=15) or left untreated (n=13) on D3, 4, 5 and harvested on D7. Lung leukocytes were analysed by flow cytometry as in Figure 1 to examine the cumulative effects of depletion. The direct, partial, and selective depletion of macrophages within 18 hours (Fig. 1) led to an indirect decline in inflammatory leukocytes. **(a)** Net changes in lung leukocyte populations. DTX treatments reduced macrophage numbers, but also led to an indirect decline in total leukocytes, eosinophils, T cells, CD11b− DCs, and CD11c+ DCs. Neutrophils were not significantly changed. **(b–c)** DTX treatment shifts the predominant phenotype of macrophages from Ly6C− CD11c+ MHCII+ to Ly6C+ CD11c− MHCII−, resembling conventional monocytes. Statistical significance was calculated using unpaired two-tailed Student's *t* test. * $p<0.05$, ** $p<0.01$, *** $p<0.001$. Results represent three independent experiments.

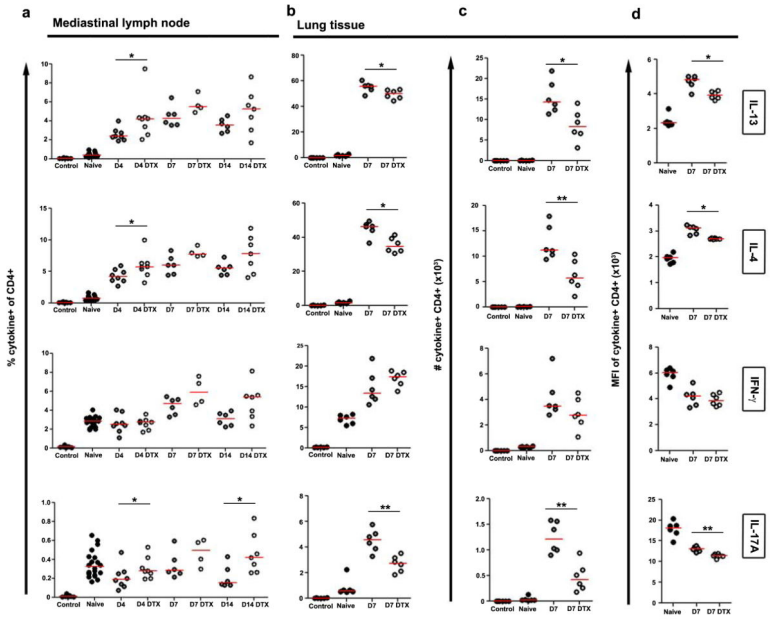

Figure 5. Reduced local but not systemic CD4+ Th2 cell responses underlie decreased lung inflammation and fibrosis

(a) Mediastinal lymph node and **(b)** lung leukocytes isolated from naïve (lymph node n=20; lung D7 n=6), egg primed and challenged (lymph node D4 n=8; D7 n=6; D10 n=6; lung D7 n=6), and primed, challenged, and DTX treated (lymph node D4 n=8; D7 n=4; D10 n=7; lung D7 n=6) CD11b-DTR mice were restimulated with PMA plus Ionomycin and stained to compare cytokine producing capabilities of CD4+ T lymphocytes. **(c)** Total numbers of cytokine-producing inflammatory CD4+ T lymphocytes in the lungs, and **(d)** magnitude of cytokine production per cell was measured by the mean fluorescence intensity (MFI) of cytokine staining. Little differences in effector CD4+ T lymphocytes were observed in lung-draining lymph nodes. In contrast DTX treatment reduced the frequency, number, and intensity of IL-13, IL-4, and IL-17A-producing CD4+ effector T lymphocytes in the lungs. Data are presented as medians. Statistical significance was calculated using Mann-Whitney U test. * $p<0.05$, ** $p<0.01$. Results represent two independent experiments.

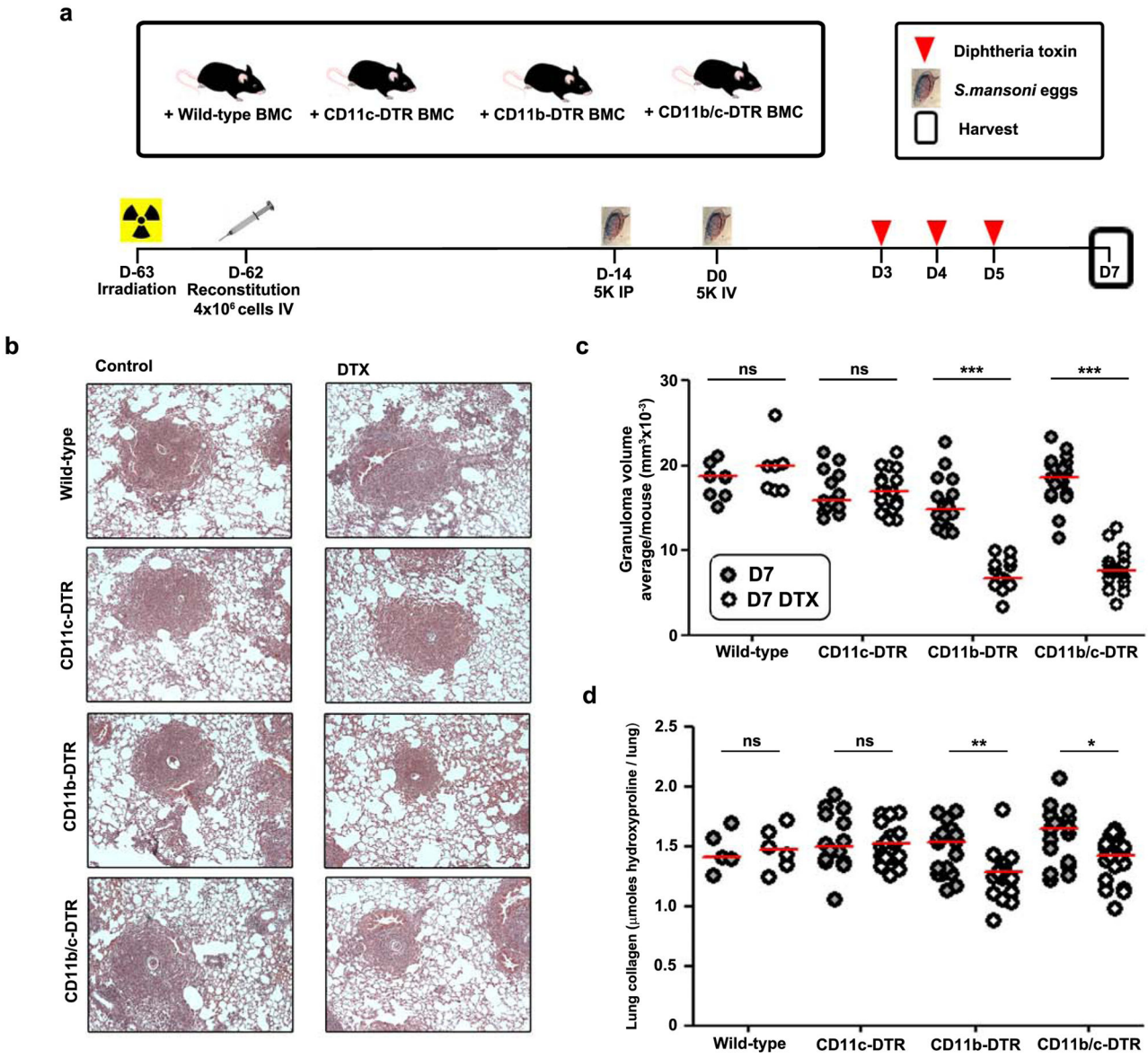

Figure 6. CD11c-DTR-sensitive leukocytes are not required after antigen priming to maintain type 2-dependent granulomas and fibrosis in the lung

(a) Wild-type C57Bl/6 mice were irradiated to ablate hematopoiesis and reconstituted with bone marrow cells from wild-type C57Bl/6, CD11b-DTR, CD11c-DTR or mice expressing both CD11b-DTR and CD11c-DTR transgenes (CD11b/c-DTR). Chimeric mice were primed and challenged with *S. mansoni* eggs, and half were treated with DTX (25ng/g) when indicated. All mice were harvested at D7. **(b)** Representative images of granulomas and collagen (blue) in lungs stained with Masson's Trichrome (wild-type control n=8; wild-type DTX n=7; Cd11c-DTR control n=14; Cd11c-DTR DTX n=18; Cd11b-DTR control n=18; Cd11b-DTR DTX n=14; Cd11b/c-DTR control n=19; Cd11c-DTR DTX n=18). **(c)** Lung granuloma volume was scored by a pathologist blinded to groups and data presented as average granuloma volume/mouse. **(d)** Lung collagen was measured by hydroxyproline content of all primed and egg challenged groups. DTX treatment of CD11b-DTR mice

reduced both secondary lung granuloma volumes and collagen content of the lung. In contrast, DTX treatment of CD11c-DTR or CD11b/c-DTR mice did not change granuloma volumes or collagen content of the lung compared to DTX treated wild-type or CD11b-DTR mice, respectively. Data are presented as median and statistical significance calculated using Mann-Whitney U test. * $p<0.05$, ** $p<0.01$, *** $p<0.001$. Results represent two independent experiments.

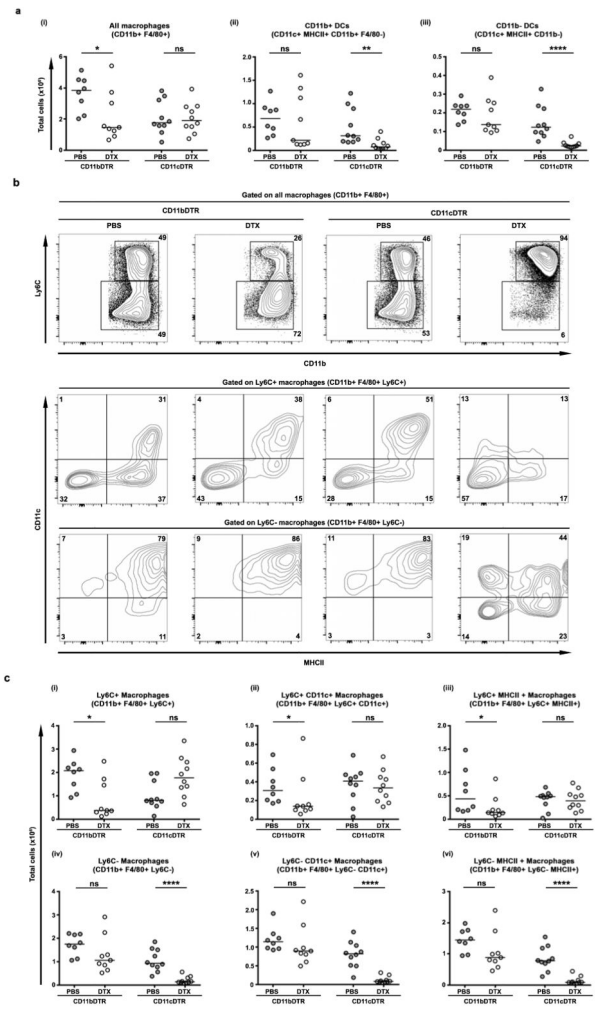

Figure 7. Failure to maintain lung inflammation and fibrosis selectively correlates with the depletion of Ly6C+ lung macrophages in CD11b-DTR mice

CD11b-DTR and CD11c-DTR egg primed and challenged transgenic mice were treated with DTX or PBS on D3 and harvested on D4. Lung leukocytes were analysed by flow cytometry to identify directly depleted cell types (CD11b-DTR PBS n=8, CD11b-DTR DTX n=9, CD11c-DTR PBS n=10, CD11c-DTR DTX n=10). **(a)** Numbers of dendritic cells and total macrophages in the lung, based on gates shown in Fig. 1a. **(b)** Reciprocal depletion of the Ly6C+ macrophage subset in CD11b-DTR and Ly6C− CD11c+ subset in CD11c-DTR mice, and profiles of CD11c and MHCII co-expression by these subsets. Percentages of gated cells from individual mice are representative or group means. **(c)** DTX treatment decreased the number of Ly6C+ macrophages in CD11b-DTR but not CD11c-DTR mice, whereas Ly6C− macrophages decreased in CD11c-DTR but not CD11b-DTR mice. Data are presented in (a) and (c) as median. Statistical significance was calculated using Mann-Whitney U test. * $p<0.05$, ** $p<0.01$, *** $p<0.001$. Results represent two independent experiments.

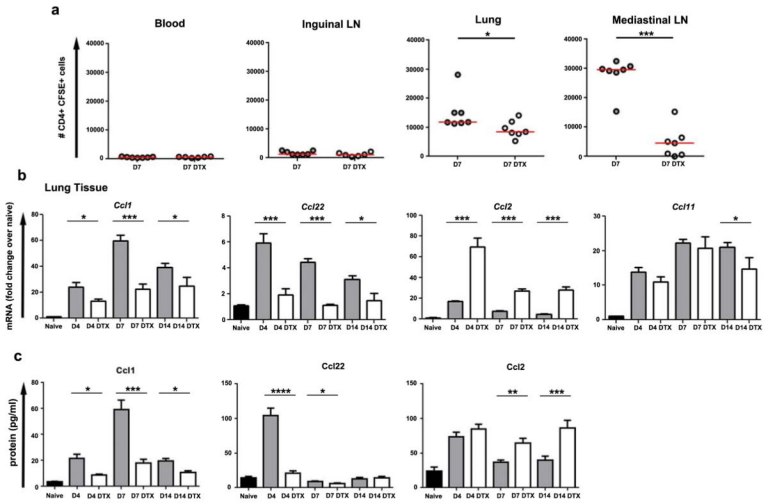

Figure 8. Macrophages regulate chemokine production and recruit effector T cells to the lungs

(a) *In vitro* activated CFSE labelled OT-II transgenic CD4+ T lymphocytes (4×10^6 cells) were injected IV into egg primed and challenged CD11b-DTR mice with or without prior DTX treatment on day 6. The homing of donor T lymphocytes was compared 24 hours after transfer by detecting CFSE+ CD4+ T cells in different tissues by flow cytometry. Fewer activated CD4+ T lymphocytes were recruited to and remained in the lung and mediastinal lymph nodes in DTX treated mice. In contrast, similar small numbers of donor cells were present in blood or inguinal lymph nodes. Relative quantitative gene **(b)** and protein expression of chemokines in lung tissue from naïve (n=13), egg primed and challenged (D4 n=8; D7 n=9, D10 n=10), and primed, challenged and DTX treated (D4 n=8; D7 n=10, D10 n=9) CD11b-DTR mice. Results were normalized to RPLP2 and scaled to naïve mice. Induction of CCL1 and CCL22 were blunted by DTX treatment while CCL2 was further increased at all time points and CCL11 remained mostly unaltered. The data in **(a)** are presented as median. The data in **(b)** and **(c)** are presented as mean ± s.e.m. Statistical significance was calculated using unpaired two-tailed Student's *t* test or Mann-Whitney U test as appropriate. * $p<0.05$, ** $p<0.01$, *** $p<0.001$. Results represent two independent experiments.

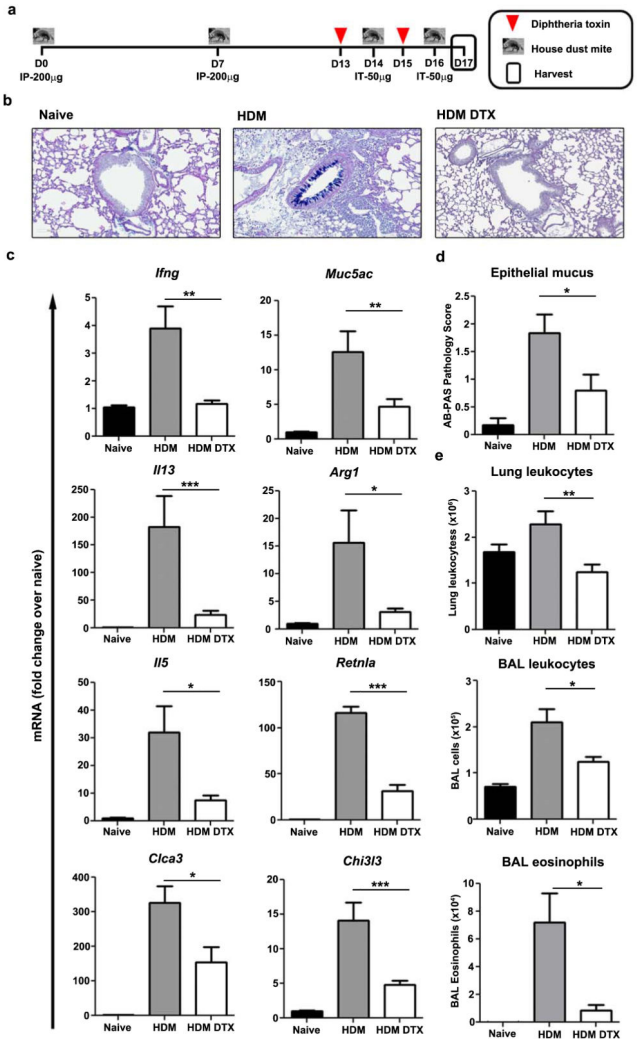

Figure 9. CD11b-DTR-sensitive cells locally drive airway allergen-induced type 2 immunity

(a) CD11b-DTR mice were primed by IP injection of house dust mite (HDM, 200μg) on D0 and 7 prior to intratracheal challenge with HDM (50μg) on D14 and 16. Half of the mice were treated with DTX (25ng/g) at D13 and 15. Lungs and lung-draining mediastinal lymph nodes were harvested on D17. **(b)** Representative images of airway epithelial mucus by Alcian blue-periodic acid-Schiff (AB-PAS) staining of saline treated (naïve n=11), HDM primed and challenged (HDM n=12), and primed, challenged, and DTX treated (HDM DTX n=10) CD11b-DTR mice. **(c)** Relative quantitative gene expression in lung tissue was normalized to RPLP2 and scaled to naïve mice. DTX treatment weakened the HDM-stimulated increase in mucus and Th2-induced genes. **(d)** AB-PAS staining (scored 0–4 by a pathologist blinded to groups) was less intense and widespread in the airways of DTX treated mice**. (e)** Total number of leukocytes in perfused lung tissue and bronchoalveolar lavage (BAL). Total number of eosinophils in BAL was calculated from cytospin analysis. DTX treatment decreased the total number of leukocytes in lung tissue and BAL, as well as airway eosinophils. Data are presented as mean ± s.e.m. Statistical significance was

calculated using unpaired two-tailed Student's *t* test. * $p<0.05$, ** $p<0.01$, *** $p<0.001$. Results represent two independent experiments.

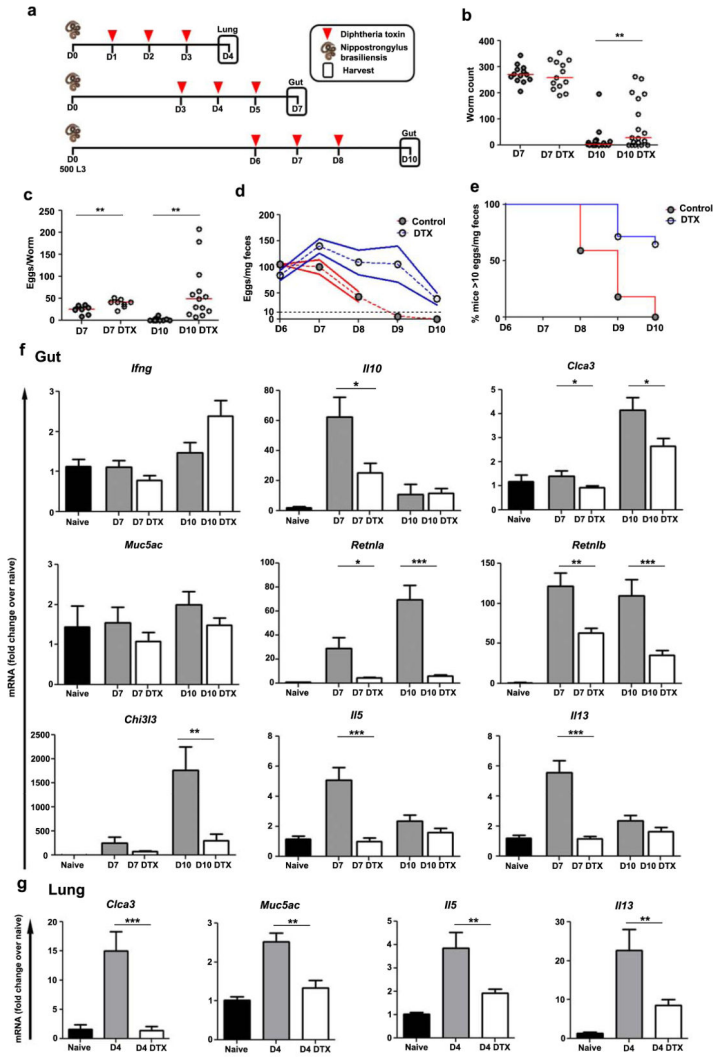

Figure 10. Macrophage depletion suppresses Th2 gene expression and impairs defense against *Nippostrongylus brasiliensis* hookworm infection

(a) CD11b-DTR mice were injected subcutaneously with *N. brasiliensis* (500 L3) at D0. Mice were harvested at D4 (lung), or 7 or 10 (gut). Half of the mice were treated with diphtheria toxin (DTX, 25ng/g) when indicated. **(b)** Intestinal worm burden was equal in control mice and DTX treated mice on D7 (n=13/group) but significantly higher in DTX mice at D10 (n=18/group). **(c)** DTX treatment increased fecundity of *N. brasiliensis* adults (eggs/worm) at both D7 and 10. Daily longitudinal fecal egg counts showed **(d)** a higher egg burden (eggs/mg feces) from D7 (n=8/group) to 10 (control n=10; DTX n=14) and **(e)** an increased percentage of infected mice above a threshold (dotted line in e) of >10 eggs/mg feces following DTX treatment (control n=22; DTX n=14). Relative quantitative gene expression in **(f)** D7 and 10 gut (grossly inflamed proximal duodenum) and **(g)** D4 lung tissue from untreated (naïve n=10), *N. brasiliensis* infected (D4 n=8; D7 n=13; D10 n=18), and infected DTX treated (DTX) (D4 n=9; D7 n=18; D10 n=28) CD11b-DTR mice. Results are normalized to RPLP2 and scaled to naïve mice. The majority of Th2-dependent genes exhibited weaker induction following DTX treatment in infected mice. The data in **(b)** and

(c) are presented as median. The data in **(d)**, **(f)** and **(g)** are presented as mean ± s.e.m. Statistical significance was calculated using unpaired two-tailed Student's *t* test or Mann-Whitney U test as appropriate. * $p<0.05$, ** $p<0.01$, *** $p<0.001$. Results represent two independent experiments.

Table 1

Gene symbol	Common name(s)	Forward Primer Sequence	Reverse Primer Sequence
Arg1	Arginase 1	GGAAAGCCAATGAAGAGCTG	GCTTCCAACTGCCAGACTGT
Arg2	Arginase 2	TCCTCCACGGGCAAATTCC	GCTGGACCATATTCCACTCCTA
CCL1	CCL1, TCA3	GGCTGCCGTGTGGATACAG	AGGTGATTTTGAACCCACGTTT
CCL2	CCL2, MCP 1	AGGTGTCCCAAAGAAGCTGTA	ATGTCTGGACCCATTCCTTCT
CCL11	CCL11, Eotaxin	GAATCACCAACAACAGATGCAC	ATCCTGGACCCACTTCTTCTT
CCL22	CCL22, MDC	TGCCATCACGTTTAGTGAAGG	CGGCAGGATTTTGAGGTCCA
Chi3l3	Ym1	CATGAGCAAGACTTGCGTGAC	GGTCCAAACTTCCATCCTCCA
Clca3	Gob5	CATCGCCATAGACCACGACG	TTCCAGCTCTCGGGAATCAAA
Ifng	IFN-gamma	AGAGCCAGATTATCTCTTTCTACCTCAG	CCTTTTTCGCCTTGCTGTTG
Il5	IL-5	TGACAAGCAATGAGACGATGAGG	ACCCCCACGGACAGTTTGATTC
Il10	IL-10	ATGCTGCCTGCTCTTACTGACTG	CCCAAGTAACCCTTAAAGTCCTGC
Il12b	IL-12/23p40	TGGTTTGCCATCGTTTTGCTG	ACAGGTGAGGTTCACTGTTTCT
Il13	IL-13	CCTCTGACCCTTAAGGAGCTTAT	CGTTGCACAGGGGAGTCTT
Il13Ra1	IL-13 receptor alpha 1	CCTGAAGGAGCCAGTCCAAA	GCCCACCTGCAGACAGATTT
Il13Ra2	IL-13 receptor alpha 2	GGAAAGGAGGACAAAGAGGTC	GATTTAGTGTGCTGAAAGCTCTACTC
Muc5ac	Muc5AC	CAGGACTCTCTGAAATCGTACCA	AAGGCTCGTACCACAGGGA
Nos2	iNOS	TGCCCCTTCAATGGTTGGTA	ACTGGAGGGACCAGCCAAAT
Retnla	RELM alpha, Fizz1	CCCTCCACTGTAACGAAGACTC	CACACCCAGTAGCAGTCATCC
Retnlb	RELM beta, Fizz2	CGTCTCCCTTTTCCCACTG	CAGGAGATCGTCTTAGGCTCTT
Rplp2	RPLP2	TACGTCGCCTCTTACCTGCT	GACCTTGTTGAGCCGATCAT